Progress in Additive Manufacturing
https://doi.org/10.1007/s40964-023-00475-y

FULL RESEARCH ARTICLE

Design guidelines for metal binder jetting

Heiko Blunk[1] · **Arthur Seibel**[1,2]

Received: 24 February 2023 / Accepted: 14 June 2023

Abstract
In addition to the general advantages of additive manufacturing technologies, such as the resource-efficient production of highly complex components, the metal binder jetting (MBJ) process enables a more cost-effective manufacturing of metal additive components. However, the design freedoms gained by additive manufacturing, and MBJ in particular, are also accompanied by new design restrictions for component design. While a large number of design guidelines are already available for the established additive manufacturing processes, the metal binder jetting process imposes additional requirements on component design, which are currently only inadequately covered in the literature. Therefore, this paper presents the development and derivation of first design rules for the metal binder jetting process using martensitic stainless steel (17–4 PH). In this way, the paper also provides a methodology for deriving guidelines regardless of the material. In total, 13 guidelines have emerged from this, which in part both confirm existing guidelines, but also extend them.

Keywords Additive manufacturing · Design guidelines · Metal binder jetting · 17–4 PH

1 Introduction

Additive manufacturing (AM) processes enable the efficient fabrication of highly complex components, but are limited in applications due to higher manufacturing costs, among other factors [1, 2]. Compared to the established metal additive manufacturing processes, the metal binder jetting (MBJ) process has significantly lower component costs, for example, 60% lower than the laser powder bed fusion of metals (PBF-LB/M) process [3, 4]. Furthermore, in comparison with metal injection molding (MIM), the MBJ process allows higher part complexity with higher cost effectiveness for lower volumes, as no tooling molds are required.

Most engineers and designers, however, are trained to design components that are manufactured using conventional processes, such as injection molding or turning. Experience with design of components for additive manufacturing as well as the boundary conditions and possibilities of the respective AM processes is only available to a small extent in comparison [5]. This leads to the fact that potentials of these manufacturing technologies are not properly raised, which may lead to increasing costs in the development, manufacturing and even use of AM components and result in a reduced acceptance and application of these technologies.

One way to avoid these costs and increase acceptance is to provide appropriate design guidelines that allow the designer to understand the process limitations and capabilities and thus exploit the full potential of the particular manufacturing process [6, 7]. Most guidelines, however, focus on the established AM technologies, such as the PBF-LB/M process [1, 8–10]. Due to the sometimes very different process characteristics, the findings cannot be directly transferred to other technologies. Since the MBJ process is still an emerging technology, the availability of design guidelines for this process and their scope are rather limited. The information provided by various manufacturing service providers [11–13] only gives an initial insight into the possibilities of the process as, for example, shown in Table 1.

In addition, there are also manufacturer-independent companies that provide design recommendations [14], which are only general in nature. For example, a minimum and maximum wall thickness are specified (0.3–20 mm), but without specifying the height or length. Furthermore, information

✉ Heiko Blunk
heiko.blunk@iapt.fraunhofer.de

Arthur Seibel
arthur.seibel@iapt.fraunhofer.de

[1] Fraunhofer Research Institution for Additive Manufacturing Technologies IAPT, 21029 Hamburg, Germany

[2] Hamburg University of Technology TUHH, 21073 Hamburg, Germany

Published online: 30 June 2023

Table 1 Basic recommendations for the MBJ process provided by Digital Metal [11]

Feature	Dimensioning
Minimum size	$1 \times 1 \times 3$ mm^3
Minimum length	1 mm
Minimum radius	35 µm
Chamfers	35 µm step size in z direction
Resolution	35 µm
Wall thickness	Preferably > 300 µm. Min. > 150 µm
Boreholes	≥ 200 µm, depending on hole depth

is given on possible overhangs, but without specifying the type and size of the overhang [12]. Other suppliers, on the other hand, refer to a minimum bore diameter of 1.5 mm, but without specifying the depth [15]. Compared with PBF-LB/M, manufacturing holes and channels with MBJ is more challenging with regard to diameter and length. The low green part strength limits the maximum component size, as otherwise complete depowdering can no longer be guaranteed. In the PBF-LB/M process, on the other hand, the maximum size is limited by the available installation space, which can be one meter and more in today's machines [16].

Apart from design guidelines, there are also design heuristics [17]. Although these already provide a good overview, they do not allow the full potential to be exploited, because the aspects are not considered in detail.

Due to the comparable process steps between metal injection molding and MBJ, general guidelines such as sinter-compatible design can be transferred from this. However, due to different process chains and the resulting difference in green part properties, a transfer of quantitative guidelines is not possible [18]. Qualitative guidelines derived from MIM include [19]:

- Use a closed footprint.
- Use transition radii.
- Avoid large volume changes.
- Avoid accumulation of material.

Despite the developments to date, there are gaps in both appropriate test geometries and guidelines. To enable wide acceptance and application of the MBJ technology, a necessary part is the provision of comprehensive design guidelines [6, 7]. To this aim, this paper presents more detailed guidelines to illustrate the process limits of this new technology. The focus is on the application of methods previously developed, the development of test geometries derived from them to take the influences in the MBJ process into account, and the determination of limit values for component design and production.

2 Materials and methods

2.1 Metal binder jetting and post processing

All green parts were manufactured using the DMP 2500 Digital Metal System. The system has drop-on-demand print heads with heating elements, which enable a resolution of 42 µm. The corresponding layer thickness is also 42 µm. To compensate for shrinkage during sintering, the component was scaled with the following factors:

X: 1.191;
Y: 1.195;
Z: 1.21.

Here, X and Y span the build plane, while Z represents the build direction. Since the scaling is used to compensate for shrinkage, all the values given refer to the unscaled test specimens.

The powder material used, 17–4 PH, was obtained from the manufacturer Digital Metal with fractions D10, D50 and D90 of 7.45 µm, 15.77 µm and 26.11 µm.

Depowdering was carried out in the manual unpacking station Depowdering Cabinet, also from Digital Metal. Using a compressed air jet, all loose powder was removed as far as possible. The compressed air nozzle is merely guided along the surfaces of the test geometries, and the nozzle is not inserted into boreholes. The powder is not removed mechanically with a brush or similar.

The components were then placed on plates of alumina with a purity of 99.5% and a porosity of 36–38% and debinded at 345 °C for two hours under ambient air.

Finally, the components were sintered at a maximum temperature of 1350 °C in an argon atmosphere with a hydrogen content of 2%. The Desktop Metal Studio System sintering furnace was used for this purpose.

2.2 Geometrical features

The process limits were determined on the basis of practical tests, which include the design, manufacturing and final geometric inspection of benchmark geometries. Based on the state of the art, previously used test specimens were considered and adapted to the process conditions of the MBJ process. In general, geometric benchmark geometries are used to evaluate the geometric performance of AM processes [20, 21]. For this purpose, various test specimens have been developed in the past and applied for different technologies [22, 23]. These are geometries that represent one or more basic geometries such as walls, boreholes and overhangs in various forms. Publications on previous design guidelines as well as various standards help in the selection of geometries. These show different

geometries that have been used for evaluation or give concrete instructions for their design. The ISO/ASTM 52910:2018 [24] standard gives assistance for exploiting the possibilities of AM processes. More details can be found in ISO/ASTM 52902:2019 [25].

Based on the previously known guidelines from the PBF-LB/M and MIM processes as well as standards, suitable basic elements were derived, which were categorized according to [8] and are shown in Fig. 1. The categories are divided as follows:

- uncurved elements (cuboids),
- single-curved elements (cylinders and boreholes),
- double-curved elements (ellipsoids).

Of these, both uncurved and single curved elements have edges that occur between two connected surfaces. A combination of connected and/or unconnected base elements leads to element transitions.

The process limits were evaluated in three successive series of tests based on the methodology from [8]. First, the individual base elements were examined in different sizes. And then, the transitions between connected and unconnected base elements were investigated.

2.2.1 Base elements

At first, the smallest manufacturable feature size was determined. For this purpose, the base elements were manufactured in different sizes from 0.05 to 1 mm and evaluated with regard to their shape and manufacturability. To facilitate handling of the base elements, they were connected to a larger base plate, as shown in Fig. 2 for the case of uncurved elements. In the case of single curved elements, cylinders are connected to the base plate instead of cuboids, and spheres in the case of double curved elements.

Larger embodiments of the uncurved and single-curved base elements were fabricated to evaluate stability during both depowdering and sintering as well as the removability of powder in relation to the aspect ratio. The geometry elements were constructed in such a way that the height was equal to an integer multiple of its width, respectively, diameter. While the cuboids were analyzed for their external

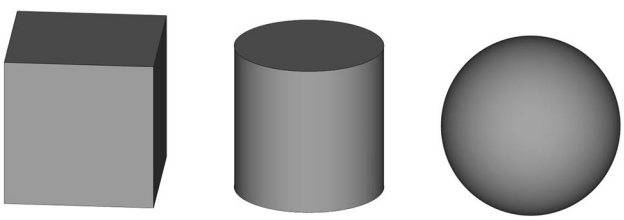

Fig. 1 Base elements for specimen design

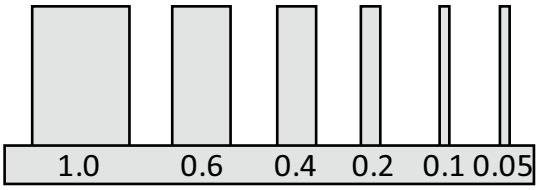

Fig. 2 Uncurved base elements including base plate and nominal width in mm

deformation, the focus for the boreholes was on complete depowdering. For this purpose, they were cut open after the sintering process and the free bore depth was determined, see Fig. 3 (right). Compared to the PBF-LB/M process, it was expected that the powder could not be completely removed from deeper boreholes, since the green parts can only be carefully depowdered due to their significantly lower strength.

The geometry and the free borehole depth were measured using the Keyence VHX 5000 digital microscope. The dimensions shown in Fig. 3 were determined within the images generated with this microscope. For the cuboids and cylinders, the difference between the base point and tip was used, and for boreholes, the maximum depth measured from the top edge to the appearance of powder that has not been removed was considered.

In addition, uncurved elements were manufactured in different orientations to analyze the influence of gravity during sintering, see Fig. 4. Four overhangs at each of four angles (30°, 40°, 60° and 90°) were manufactured and analyzed. The thickness was set to 1 mm. While in the PBF-LB/M process the overhang angle has an influence on the surface roughness and the need for support structures, in the MBJ process it is mainly the influence of gravity during sintering that has to be determined. Due to the good support effect of the powder, no support structures were required during the printing process.

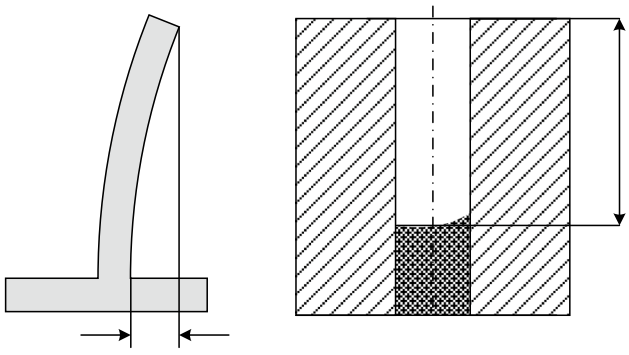

Fig. 3 Measured variables for determining the deformation of uncurved and single-curved elements (left) and the free bore depth (right)

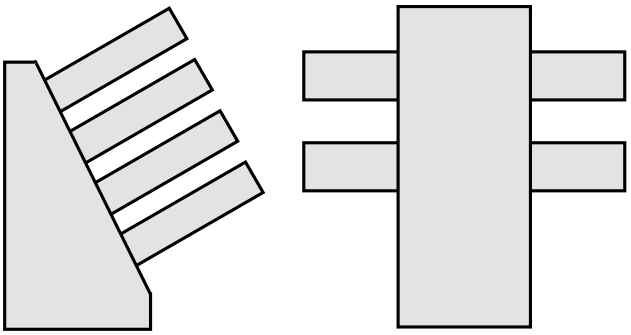

Fig. 4 Side view of the test geometry for evaluating uncurved base elements with an overhanging angle of 60° (left) and 90° (right)

For the examination of the basic elements, each test specimen was manufactured four times.

2.2.2 Edges

Furthermore, the edge sharpness was evaluated based on two test geometries, one of which has six inner and the other six outer edges, see Fig. 5. Both geometries were designed without radii. After sintering, they were cut in the center to prevent unwanted rounding while handling during production from being included in the measurement results. The cross sections were then evaluated using the VHX 5000 digital microscope from Keyence. For this purpose, the radius of a circle that runs along the component contour at the respective edges was determined.

2.2.3 Element spacing

Another characteristic of the MBJ process is that the powder bed provides sufficient support during the printing process, thus eliminating the need for support structures. This means that components can be stacked or nested more easily. The closer the components are to each other, the greater is the utilization of the installation space, which significantly reduces production costs [4]. To evaluate whether the component spacing is still sufficient, both uncurved and single-curved elements were placed at different orientations and different distances from each other (see Fig. 6) and attempts were made to separate them during the depowdering process. The evaluation of sufficient spacing between elements was done objectively according to the separability of the two test specimen segments. If the two halves could be separated from each other without force or destruction, the existing gap width was assumed to be suitable. To investigate the influence of orientation, the orientation of the cleavage plane and cleavage axis was chosen both horizontally and vertically as well as inclined at 45° to the direction of buildup.

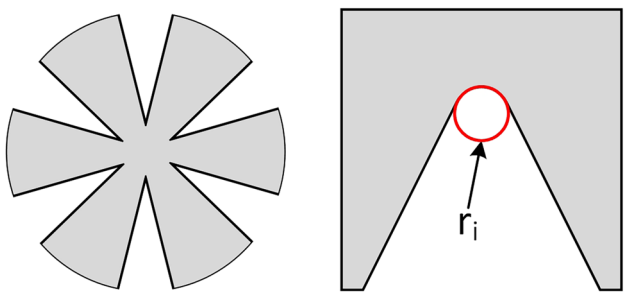

Fig. 5 Top view of the test geometries for investigating inner edges (left) and measuring principle (right)

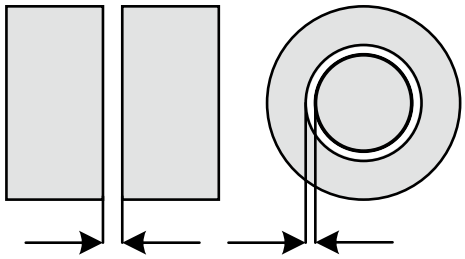

Fig. 6 Top view of the test geometries for examining element spacing

3 Results and discussion

3.1 Base elements

3.1.1 Size

The evaluation of the feature size basically shows that, regardless of the base element, manufacturing with an edge length or diameter of ≤ 0.1 mm could not be successfully realized. Either the elements were not successfully built (single- and double-curved) or the size of the element significantly deviated from the CAD geometry. While the required dimensional specifications could be achieved for a width of 0.2 to 1 mm, the actual width of approx. 0.18 mm is around 80% larger than the target width of 0.1 mm, which is around the magnitude of two pixels. This deviation can be attributed to the characteristics of the printing process. During data preparation, the component contours of the individual layers are approximated by pixels. It can happen that there is only a partial overlap between contour and pixel. However, such pixels were printed completely, which means that the contour tends to be printed larger than intended in the CAD model. When comparing with the data in Table 1 (minimum size), it should be noted that, although smaller sizes were obtained, there is also a minimum practical size at which the component can still be handled. Therefore, these values should be considered as minimum sizes for features and not for stand-alone components. With regard to the minimum

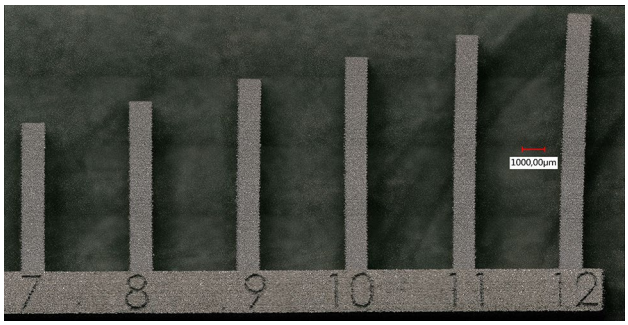

Fig. 7 Uncurved elements with an aspect ratio of 7–12

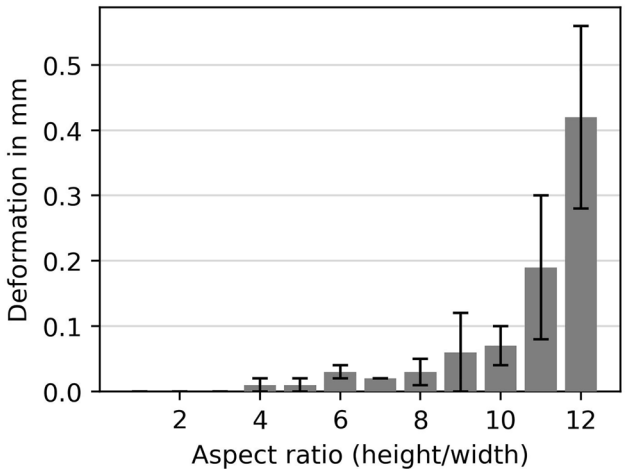

Fig. 8 Deformation as a function of aspect ratio for uncurved specimens at 0° orientation

wall thickness, both the cited and the determined values were in the same range. Single and double curved elements, however, have a larger minimum dimension. The cylindrical base elements could only be successfully built up from a diameter of 0.2 mm and the double-curved elements from a diameter of 0.4 mm.

3.1.2 Aspect ratio

After sintering of the test geometries, there was already a clear difference visible between a low and a high aspect ratio, see Fig. 7. For example, while no deformation is visible to the bare eye at a ratio of seven, a ratio of 12 shows a clearly visible deformation.

This is also reflected in the measured values, which are shown in Fig. 8. Increasing aspect ratio is accompanied by greater deformation. Up to an aspect ratio of eight, the deformation can still be considered tolerable, which is thus in a similar size range to the print resolution [11] and in the same range as given for metal material extrusion [14]. It is,

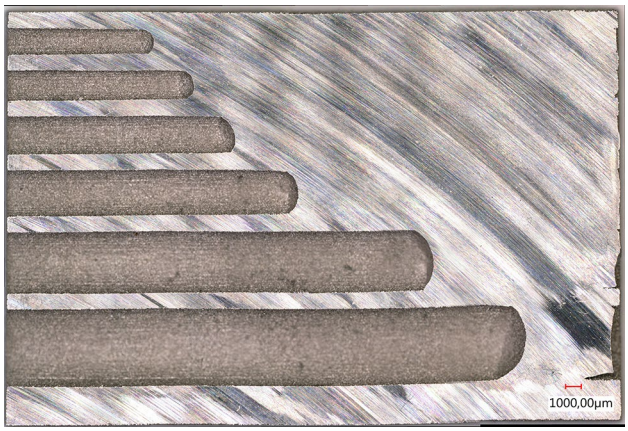

Fig. 9 Sectional view of manufactured boreholes with different diameters and remaining powder

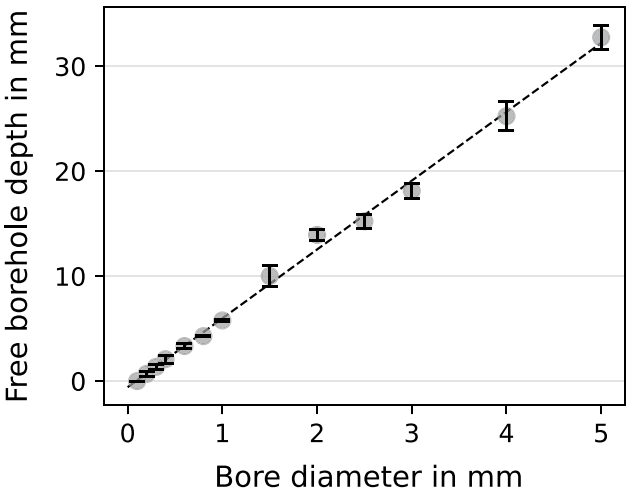

Fig. 10 Depowdered borehole depth as a function of the bore diameter

therefore, becoming apparent that this value is independent of the process used to produce the green part. The extent to which this also applies to other materials, such as copper or titanium, remains to be investigated.

3.1.3 Boreholes

As previously described, the test specimens of the depowered boreholes were cut open in the center after sintering to evaluate the removability of the powder. As shown in Fig. 9, the free hole depth increases with increasing diameter. In addition, most of the powder could be removed in the center of the hole, while slightly more powder remains in the area of the walls.

As shown in Fig. 10, there is an almost linear relationship between the free bore depth and its diameter. Whereas with a

bore diameter of 0.2 mm the powder could be removed to a depth of approx. 0.7 mm, with a diameter of 5 mm this was already possible to a depth of 33.8 mm. Below a diameter of 0.2 mm, no powder could be removed from the borehole. This confirms Digital Metal's lower limit of 0.2 mm for manufacturable hole diameters. In addition, it can be stated that, in the case of blind holes, these can be successfully depowdered and thus manufactured up to six times the hole diameter. Due to the accessibility from both sides for through holes, this value doubles to 12. However, powder can be removed from larger depths when the depowdering nozzle is inserted into the borehole. With a nozzle length of approx. 20 mm, it was possible to remove the powder from a borehole with a diameter of 1 mm to a depth of approx. 25 mm, instead of only from a depth of up to 5.8 mm.

3.1.4 Overhangs

As in Section "Aspect Ratio", uncurved overhangs also show a stronger deformation with increasing overhang length and angle. While significant deformations are present for vertically oriented elements only from an aspect ratio of about nine, they occur earlier for overhanging elements, as expected. Depending on the angle, the ratio at which significant deformation (> 1 pixel) occurs is three for a 90° overhang and four for an overhang of 30°, 40° and 60°, see Fig. 11.

3.2 Edges

During manufacturing of the test geometries for evaluating inner and outer edges, no defects such as cracks or similar were found in the test specimens. Likewise, despite the different orientation of the individual edges in the build plane, no obvious differences could be seen between the characteristics of the individual edges. This is also reflected in the measured values of the individual radii shown in Table 2. Although there is a comparatively high standard deviation, the values do not show any dependence on the orientation in the construction plane. It can be seen that the inner radii at about 60 µm tend to have a larger minimum radius than the outer radii at about 50 µm. Both radii are larger than specified in the state of the art. This may be related to either the printing parameters or the material used. Further tests are required to be able to assess this conclusively.

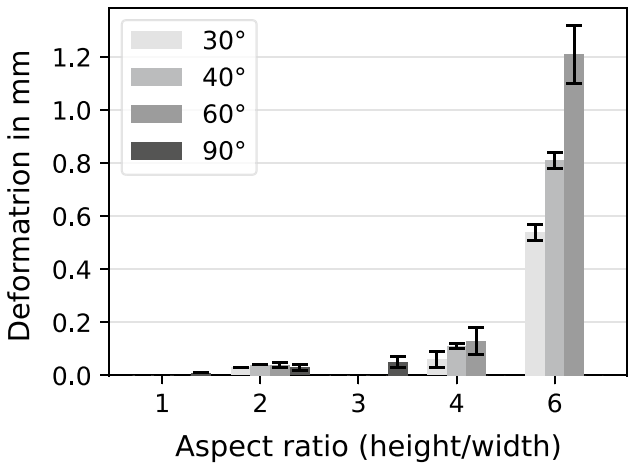

Fig. 11 Deformation as a function of aspect ratio for uncurved specimens at various orientations

Table 2 Achievable edge sharpness for inner and outer edges

Specimen number	Inner radius in µm	Outer radius in µm
1	53.30	31.40
2	70.99	75.90
3	80.75	40.81
4	42.50	52.11
5	64.51	51.01
6	51.15	49.66
Mean	60.53	50.15
Standard deviation	14.14	14.88

3.3 Element spacing

The evaluation of transitions between unconnected base elements shows that the gap width can be chosen smaller for uncurved elements than for curved ones, see Table 3. From a gap width of 0.09 mm, uncurved elements can be separated without force or damage. For single-curved elements, the required minimum gap width of 0.2 mm is more than twice as high. These limits were observed for all four samples. As with feature size, this difference can be attributed to the approximation of the CAD geometry by pixels. This results

Table 3 Evaluation results for element spacing

Element type	Spacing in mm	Horizontal	Vertical	45°
Uncurved	0.04	x	x	x
	0.05	x	x	x
	0.09	✓	✓	✓
	0.13	✓	✓	✓
	0.20	✓	✓	✓
Single-curved	0.05	x	x	x
	0.09	x	x	x
	0.13	x	x	x
	0.20	✓	✓	✓

in smaller inner diameters and larger outer diameters, making the gap smaller during the printing process.

4 Conclusion and outlook

The investigations have shown that the process limits of the metal binder jetting process can be clearly identified under the conditions presented. As expected, these differ from other metal additive manufacturing processes, such as PBF-LB/M. In PBF-LB/M, for example, it is possible to build walls from a width of approx. 1.5 mm higher than 80 mm without defects [1], whereas in metal binder jetting the maximum height is limited to eight times the width.

Based on the measurement results, the following process limits can be established:

4.1 Cuboids

- Minimum edge length: 0.1 mm
- Ratio of height to minimum edge length: 8

4.2 Holes

- Minimum diameter: 0.2 mm
- Ratio depth to diameter blind holes: 6
- Ratio depth to diameter through holes: 12

4.3 Cylinders

- Minimum diameter: 0.2 mm

4.4 Ellipsoids

- Minimum inner radius: 0.4 mm
- Minimum outer radius: 0.4 mm

4.5 Overhangs

- Ratio of length to height: 1

4.6 Edges

- Minimum transition radius (inner radius): 0.06 mm
- Minimum edge fillet (outer radius): 0.05 mm

4.7 Element spacing

- Minimum distance uncurved: 0.1 mm
- Minimum distance single-curved: 0.2 mm
- Minimum distance double-curved: 0.2 mm

However, the presented design guidelines represent only a part of the process boundaries. Further characteristics and combinations of basic elements must be analyzed to identify further limits. For example, it remains to be investigated whether the limits for the determined aspect ratios from feature height to thickness or from overhang length to thickness for uncurved elements also apply to single-curved elements. It should also be noted that the investigations were carried out with the material 17–4 PH. The extent to which the results can be transferred to other materials remains to be investigated. The described methodology, however, should be transferable to other materials.

As a first step towards digitizing the guidelines, they could be implemented in software that checks components for compliance with these rules. This would enable critical components or component areas to be identified more quickly.

Acknowledgements The research was funded by Hamburgische Investitions- und Förderbank (IFB Hamburg) in the project "PuMa—Entwicklung einer prototypischen Softwarelösung zur Vorhersage und Kompensation des Bauteilverzuges beim Sintern von Metall-Binder-Jetting (MBJ)-Bauteilen sowie einer effizienten Nachbearbeitungs- und Qualifizierungsstrategie".

Funding Open Access funding enabled and organized by Projekt DEAL.

Data availability The experimental data can be provided upon request by the authors.

Declarations

Conflict of interest On behalf of all authors, the corresponding author states that there is no conflict of interest.

References

1. Kranz J (2017) Methodik und Richtlinien für die Konstruktion von laseradditiv gefertigten Leichtbaustrukturen. Springer, Berlin, Heidelberg
2. Berger R (2019) Additive manufacturing-Taking metal 3D printing to the next level. https://www.slideshare.net/MartinErharter/additive-manufacturing-takingmetal-3-d-printing-to-the-next-level-study-by-roland-berger-200943228. Accessed 27June 2023

3. Digital Alloys. (2019). Guide to Metal Additive Manufacturing – Part 5 – Economics of Metal Additive Manufacturing. https://www.digitalalloys.com/blog/economics-metal-additive-manufacturing. Accessed 27 June 2023
4. AMPOWER GmbH & Co. KG (2018) Metal Additive Manufacturing with sinter-based technologies [White paper]. https://ampower.eu/insights/additive-manufacturing-sinter-based-technologies/. Accessed 27 June 2023
5. Emmelmann C, Herzog D, Kranz J (2017) Design for laser additive manufacturing. Laser Additive Manufacturing. Woodhead Publishing, London, pp 259–279
6. Seepersad CC, Allison J, Sharpe C (2017) The need for effective design guides in additive manufacturing. In: DS 87-5 Proceedings of the 21st international conference on engineering design (ICED 17), Vol 5: Design for X, Design to X. Vancouver, Canada, pp 309–316
7. Kranz J, Herzog D, Emmelmann C (2015) Design guidelines for laser additive manufacturing of lightweight structures in TiAl6V4. J Laser Appl 27(S1):S14001
8. Adam G (2015) Systematische Erarbeitung von Konstruktionsregeln für die additiven Fertigungsverfahren Lasersintern, Laserschmelzen und Fused Deposition Modeling. Shaker Verlag, Aachen
9. Wang P, Song J, Nai MLS, Wei J (2020) Experimental analysis of additively manufactured component and design guidelines for lightweight structures: a case study using electron beam melting. Addit Manuf 33:101088
10. Mani M, Witherell P, Jee H (2017) Design rules for additive manufacturing: a categorization. In International Design Engineering Technical Conferences and Computers and Information in Engineering Conference vol 58110. American Society of Mechanical Engineers. pp V001T02A035
11. Digital Metal (2021) DM P2500-3D metal printing at its best. https://digitalmetal.tech/printer-line/design-and-function. Accessed 17 June 2021
12. The ExOne Company (2020) 2020 Metal 3D printing manufacturing design guidelines. https://www.exone.com/Admin/ExOne/media/Documents/Mfg-Guidelines-Download-Updated-04142020-NEW.pdf. Accessed 27 June 2023
13. Materialise (2023) Konstruktionsrichtlinien Aluminium 3D Metalldruck, https://www.materialise.com/de/academy/industrial-academy/design-additive-fertigung. Accessed 6 June 2023
14. AMPOWER GmbH & Co. KG (2021) Design guidelines for sinter-based Additive Manufacturing [White paper]. https://ampower.eu/insights/design-guideline-for-sinter-based-additive-manufacturing/. Accessed 27 June 2023
15. 3D HUBS B.V. (2023). How to design parts for binder jetting 3D printing. https://www.hubs.com/knowledge-base/how-design-parts-binder-jetting-3d-printing/#design. Accessed 25 Apr 2023
16. Dahmen T, Klingaa CG, Baier-Stegmaier S, Lapina A, Pedersen DB, Hattel JH (2020) Characterization of channels made by laser powder bed fusion and binder jetting using X-ray CT and image analysis. Addit Manuf 36:101445
17. Klein Blösch A (2020) Design Heuristics for Additive Manufacturing. Dissertation, ETH Zürich
18. Blunk H, Seibel A (2023) Toward a design compendium for metal binder jetting. Innovative product development by Additive Manufacturing 2021. Springer, Cham, pp 39–48
19. Heaney DF (2019) Designing for metal injection molding (MIM). Handbook of metal injection molding. Woodhead Publishing, London, pp 25–43
20. Rebaioli L, Fassi I (2017) A review on benchmark artifacts for evaluating the geometrical performance of additive manufacturing processes. Int J Adv Manuf Technol 93(5):2571–2598
21. Mahesh M (2004) Rapid prototyping and manufacturing benchmarking. PhD Thesis, National University of Singapore
22. Digital Metal (2019) Additive manufacturing of small and complex metal parts. Höganäs AB, Höganäs
23. Shah P, Racasan R, Bills P (2016) Comparison of different additive manufacturing methods using computed tomography. Case Stud Nondestruct Test Eval 6:69–78
24. ISO/ASTM 52910:2018-07, Additive Fertigung—Konstruktion—Anforderungen, Richtlinien und Empfehlungen
25. ISO/ASTM 52902:2019-07, Additive Fertigung—Testkörper—Allgemeine Leitlinie für die Bewertung der geometrischen Leistung additiver Fertigungssysteme (AM-Systeme)